Fatigue behaviour of underclad cracks in reactor vessel nozzles

J.L.Bernard, J.Vagner & A.Pellissier-Tanon
Framatome, Paris La Défense, France

ABSTRACT

In 1979 underclad cracks were found in the HAZ of pressurized water reactor vessel nozzles. A safety analysis performed with conservative hypothesis on crack sizes, stresses and materials properties has shown that no crossing of underclad defects through the cladding is to be expected with 40 years of operating life and that the final dimensions of the defects are much less than the critical size calculated from the toughness of the material.

At the same time an experimental programme on large specimens containing actual and artificial defects was undertaken in several laboratories. The main results are the following :

- numerical simulations of crack growth agree well with experimental measurements,
- there exists a significant initiation time which is necessary before the defects propagate like fatigue cracks,
- the absence of air or agressive environment in the defects induces a significant decrease in the FCGR when compared to the behaviour in air.

By introducing in the analysis the crack initiation time and reduction of FCGR for embedded cracks it follows that the actual growth of underclad cracks in nozzles will be negligible for the in-service conditions.

1 INTRODUCTION

In 1979 cracks were found in the heat affected zone under the stainless steel cladding of pressurized water reactor nozzles. A safety analysis was performed in particular for the highest stressed zone of the nozzle corner with upper bounds taken for the variables : crack sizes, number of occurence of the transients, crack growth rate laws ; and lower bounds for toughness and tensile properties.

The main conclusions of this safety analysis were that no crossing of underclad deffects through the cladding is to be expected with 40 years of operating life and the final dimensions of the defect are much less than the critical size calculated from the toughness of the material.

At the same time an experimental programme on large specimens containing defects was undertaken in several laboratories : i) to verify the conservatism of the analysis and ii) to evaluate the margins between actual and predicted crack growth behaviour.

In this paper the main results are presented and discussed.

2 EXPERIMENTAL PROGRAMME

The mock-ups tested were taken out of an actual nozzle in A 508 C13 containing underclad cracks in the HAZ under the three layer cladding 309 L/ 308 L. The mock-ups geometries are given in fig. 1. The central part was extracted from the nozzle and heads were welded on this part for gripping in the testing machine.

Two types of specimens were tested :

1. specimens with actual embedded underclad cracks in the HAZ,
2. specimens with through thickness strip underclad cracks simulated by electro-erosion machined slots.

The initial embedded crack geometry can be represented by ellipses with typically $\frac{a}{c} \simeq \frac{1}{5}$.

During fatigue, testing X rays examinations have been used to follow the crack propagation of embedded defects and a travelling microscope was used for through thickness artificial defects. Beach marks which appear when tests are interrupted were also used to measure the crack growth.

Tests parameters (temperature, σ_{max} , load ratio R) have been determined in order to simulate the main transients : cold hydro-test, load follow (15-100 %), heat up/cold down.

3 RESULTS OF TESTS

3.1 Fatigue crack initiation on defects

An important feature of the underclad crack behaviour is that a significant fraction of lifetime is spent before crack initiation, which is not allowed for in predictive evaluations. This neglecting of initiation period results in a considerable underestimate in viable life. It has been found that a period extending between $\frac{Nf}{4}$ and $\frac{Nf}{3}$ (where Nf is the number of cycles to complete failure) was necessary before crack growth begins. This fact was deduced :

1. from accurate radiographic examinations during interruption of tests,
2. from beach marks resulting from interruption of tests,
3. from detection of crack initiation by accoustic emission techniques supported also by SEM examination on the fracture surface.

A good agreement (typically 15-20 % of number of cycles) has been found between the early growth detected by radiographic examination, the apparition of beach marks on the fracture surface and accoustic emission.

It has been found from accoustic emission measurements that crack initiation occured first in the base metal. The block diagram of the electronic system is presented in fig. 2. A typical record of the summation of accoustic emission counts is represented in fig. 3. During 10^5 cycles a significant accoustic emission occurs which is attributed to localized fatigue crack initiations on geometrical irregularities of the defect front. This emission diminishes until 3×10^5 cycles when again a significant increase is noted. From X rays and SEM examinations this increase could be related to fatigue crack initiation in the base metal. After that, a new increase of accoustic emission could be related to crack initiation in the cladding.

3.2 Environmental effects

A particular feature to be noted for underclad cracks which are primitively embedded is that fracture surface aspect changes after the crack has reached the free surface of the cladding or base metal. Before that, the fracture surface is not well defined and looks like fractures obtained in vacuum or inert environment (Hudson 1970), (Mahoney 1974), (James 1976). Afterwards, clearly defined fatigue situations immediately appear. These two aspects are shown in fig. 4. Analysis of results (see § 3.3) reveals also the different behaviours of crack propagation between actual embedded cracks without external contact and artificial through thickness cracks in contact with air at 300 °C.

3.3 Results and analysis of fatigue crack propagation tests

Numerical simulation of the crack growth, begining after the crack initiation period have been performed in order to analyse the results. Such simulations provide a basis to estimate the margins taken in the crack propagation computation in the safety analysis.

The procedure was as follow :

- for each case, the crack is supposed to be initiated and to propagate both in base metal and stainless steel cladding,
- the numerical simulation is performed by using upper bounds and lower bounds of crack growth rate data in air available for the two materials, the equations used for these curves are given in Table I,
- stress intensity factors for elliptical cracks (case of embedded actual defects) and for through thickness articicial defects have been computed by using the formulations given by (Tada 1979),
- the effects of residual stresses have been considered as negligible at 300 °C in agreement with strain gages measurements and computational results which showed that the residual stresses in the cladding and base metal are just annuled by the effect of differential thermal expansion when heating at the test temperature (300 °C).

TABLE I : Fatigue crack propagation laws used for numerical simulations

Cladding (300°C)	upper bound	$da/dN = 7.5 \times 10^{-10} \left(\frac{\Delta K}{1-\frac{R}{2}}\right)^4$ for all ΔK
	lower bound	$da/dN = 1.3 \times 10^{-10} \left(\frac{\Delta K}{1-\frac{R}{2}}\right)^4$ for all ΔK (mm/cycle, ΔK in MPa$\sqrt{m}$)
A 508 Cl 3 base metal 300°C	upper bound	$da/dN = 7.95 \times 10^{-9} \left[K_{max} (1-R)^{0.75}\right]^{2.93}$ for $\Delta K \leq 20$ MPa$\sqrt{m}$ $da/dN = 2.6 \times 10^{-8} (\Delta K)^{2.67}$ for $\Delta K > 20$ MPa$\sqrt{m}$
	lower bound	$da/dN = 3.80 \times 10^{-9} \left[K_{max} (1-R)^{0.75}\right]^{2.93}$ for $\Delta K \leq 20$ MPa$\sqrt{m}$ $da/dN = 1.5 \times 10^{-8} (\Delta K)^{2.67}$ for $\Delta K > 20$ MPa$\sqrt{m}$

Typical experimental and predicted crack growth curves are given in figures 5 to 7.

It appears that :

i) crack growth of embedded cracks are overestimated by the use of the model described above,

ii) crack growth of through thickness artificial cracks can be correctly described by the model above.

One can notice that using an other set of reference curves (Rungta 1986) leads to similar results.

The results on embedded cracks show that their crack growth rate is lowered when compared to the behaviour in air. This was also observed by (Schijve 1977) for internal cracks in an aluminium alloy. In order to account for this crack growth lowering, reductions of a factor of 4 and 3 were applied respectively to the FCGR of the cladding and the base metal. The choice of these ratio is substantiated by results of FCGR studies in vacuum on the two materials and from several data in litterature (Smith 1969), (Cooke 1975), (James 1976), (Mahoney 1974), (Bowen 1985).

4 ASSESSMENT OF MARGINS IN THE SAFETY ANALYSIS

The safety calculations have been performed with the following conditions :

- upper bounds of crack growth laws in air environment have been used for both the base metal and the cladding,
- fatigue crack initiation on the actual underclad defects has not been taken into account,
- the crack lengths have been corrected using the Irwins's correction which account for the plastic zone sizes at the crack tips,
- elliptical defects have been considered as strip defects.

Figures 8 and 9 show actual and predicted crack growth considering safety type predictions (case 1) and a realistic crack growth prediction taking into account realistic shapes and favourable environmental effects, but no crack initiation time.

The margins can be evaluated by considering the ratios :

actual life/life (case 1) (typically 10-15)
and actual life/life (case 2) (typically 2-4)

We can observe that considerable margins are existing between actual growth and predicted growth using conditions of the safety analysis. Particularly the number of cycles to have the crack breaking through the cladding with the conditions of the safety analysis is lower than actual number of cycles for crack initiation.

5 CONCLUSIONS

An extensive programme has been undertaken in order to study the initiation and fatigue crack propagation of both artificial through thickness underclad defects and actual embedded underclad defects.

Accurate crack growth measurements have been performed during the tests by using radiographic, optical microscopic and SEM examinations.

Special features of underclad crack behaviour have been pointed out :

- a significant initiation period is necessary before the internal defects propagate like fatigue cracks,

- there are evidences that the absence of air or agressive medium in the defects induces a decrease in crack growth rate when compared to air results.

Fatigue crack growth of both through thickness artificial and actual embedded underclad defects can be correctly predicted by using a model which takes mainly into account, the defect geometry, the fatigue properties relevant to the actual environmental conditions of the A 508 C1 3 base metal and the 309 L/308 L cladding.

The results show that very large margins exist between the actual crack growth and the prediction made for the safety analysis.

It follows that the actual growth of underclad defects in nozzles will be negligible for the in-service conditions.

REFERENCES

Hudson, C.H., Seward, S.K. 1970. A litterature review and inventory of the effets of environment on the fatigue behaviour of metals. Engineering Fracture Mechanics, Vol. 8.

Mahoney, M.W., Paton, N.E. 1974. The influence of gas environment on fatigue crack growth rates in types 316 and 321 stainless steels. Nuclear Technology, Vol. 23.

James, L.A. 1976. Fatigue crack propagation in austenitic stainless steels, Atomic Energy Review, 14-1, pp 37-86.

Tada, H. 1973. The stress analysis of cracks handbook. DEL Research corporation, Hellertown, Pennsylvania.

Rungta, R., Mindlin, H., Gilman, J.D. 1986. Application of EPRI data base on environmentally assisted cracking in the nuclear industry. Materials Performance, Nov, pp 43-52.

Schijve, J. 1978. Internal fatigue cracks are growing in vacuum. Engineering Fracture Mechanics, Vol. 10, pp 359-370.

Smith, H.H, Shahinian, P., Achter, M.R. 1969. Fatigue crack growth rate in type 316 stainless steel at elevated temperature as a function of oxygen pressure. Transactions of the metallurgical society of AIME, Vol. 245, May, pp 947-953.

Cooke, R.J., Irving , P.E., Booth, G.S., Beevers, C.J. 1975. The slow fatigue crack growth and threshold behaviour of a medium carbon alloy steel in air and vacuum. Engineering Fracture Mechanics, Vol. 7, pp 69-77.

Bowen, P., Knott, J.F. 1985. Effects of segregation and environment on fatigue crack growth at elevated temperature. Proc. 7th Int. Conf. on the strength of metals and alloys. Montreal, Canada, Pergamon Press, pp 1305-1310.

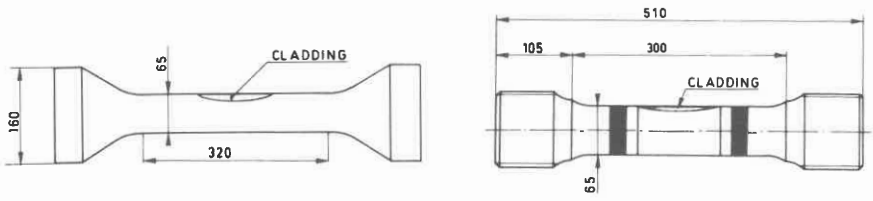

FIGURE 1 ; Specimens geometries

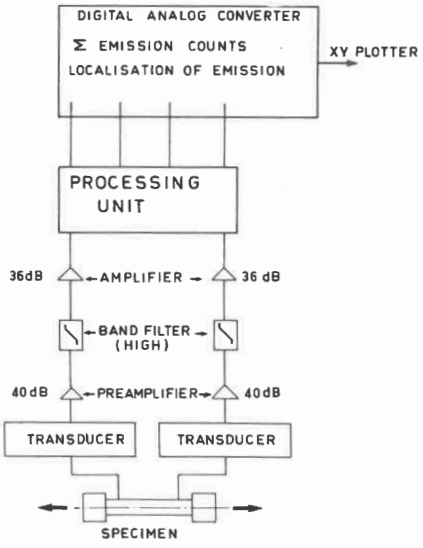

FIGURE 2 : Block diagram of the electronic system for detection of accoustic emission

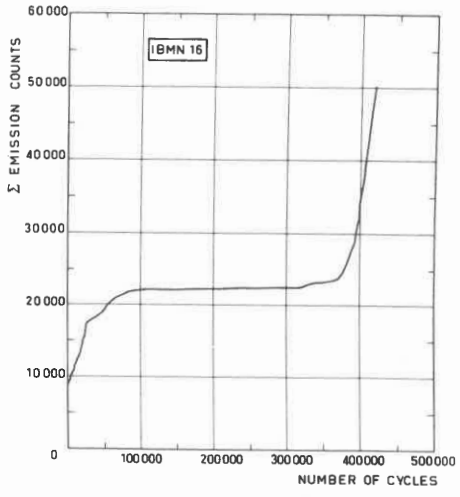

FIGURE 3 : Typical record of the summation of emission counts during a test

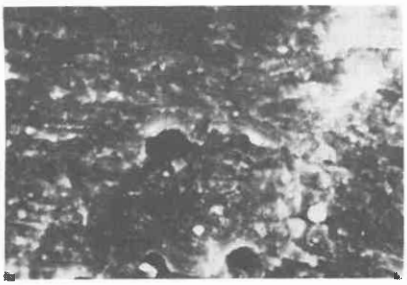

Embedded fatigue crack (a)

0,005 mm

Well defined striations (external fatigue crack)

0,005 mm

FIGURE 4 : Difference of fatigue surface aspect before (a) and after (b) the crack has reached the surface of specimen

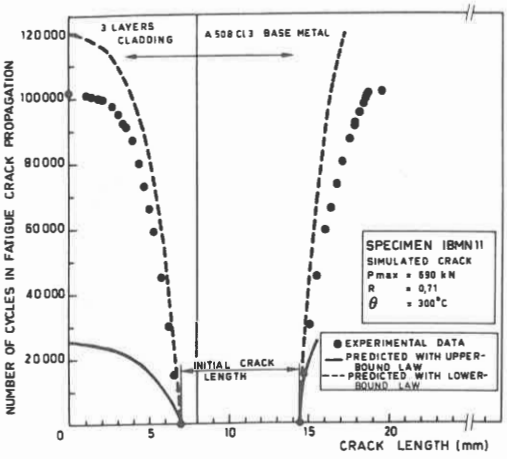

FIGURE 5

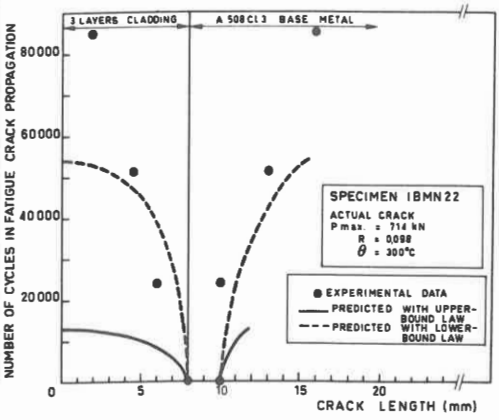

FIGURE 6

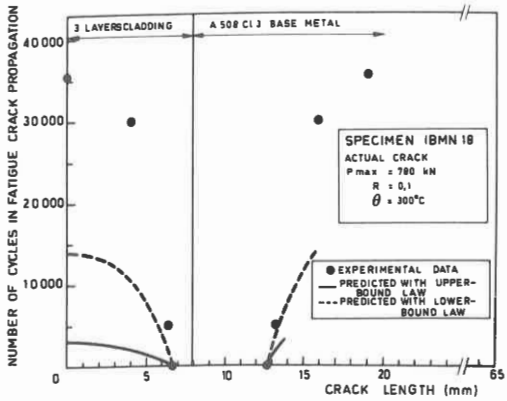

FIGURE 7

FIGURES 5-6-7 : Actual and artificial underclad defects Comparisons between actual and predicted crack growths

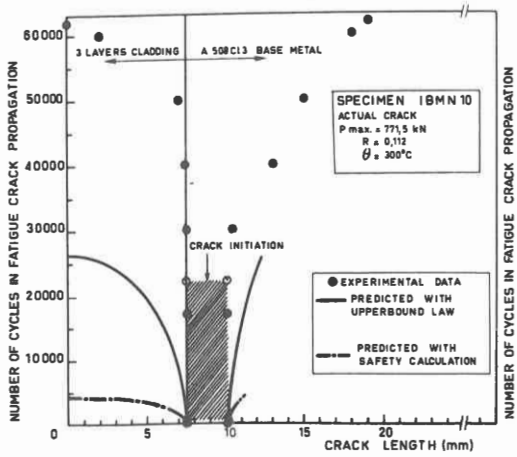

FIGURE 8

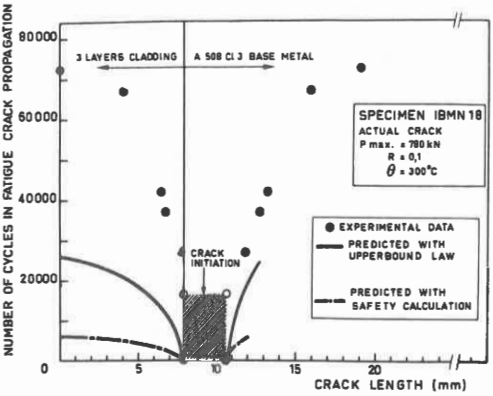

FIGURE 9

FIGURES 8-9 : Comparisons between actual and predicted crack growths of underclad defects with realistic crack growth laws and safety hypothesis